

AN INTEGRATED APPROACH TO ASSESSING THE FRACTURE SAFE MARGINS OF FUSION REACTOR STRUCTURES

G. R. Odette (Department of Mechanical Engineering and Department of Materials, University of California, Santa Barbara)

SUMMARY

Design and operation of fusion reactor structures will require an appropriate data base closely coupled to a reliable failure analysis method to safely manage irradiation embrittlement. However, ongoing irradiation programs will not provide the information on embrittlement necessary to accomplish these objectives. A new engineering approach is proposed based on the concept of a master toughness-temperature curve indexed on an absolute temperature scale using shifts to account for variables such as size scales, crack geometry and loading rates as well as embrittlement. While providing a simple practical engineering expedient, the proposed method can also be greatly enhanced by fundamental mechanism based models of fracture and embrittlement. Indeed, such understanding is required for the effective use of small specimen test methods, which is a integral element in developing the necessary data base.

INTRODUCTION

Design and operation of fusion reactors will require quantitative predictions of in-service degradation of a wide range of mechanical properties. For defect tolerant structural designs, the maximum allowable stresses and strains will often be dictated by the sizes and configurations of cracks that develop (or are presumed to develop) in service and the effective fracture toughness of the structural material. In this context, the effective fracture toughness (K_e) is defined as an engineering parameter that can be used in a structural mechanics analysis to determine the stresses (loads) and strains (load point displacements) resulting in unstable extension of a plane strain Mode I fatigue (sharp) crack of specified size and geometry. Since it may increase the probability of such rapid failures, irradiation induced degradation of fracture toughness, or embrittlement, has been identified as one of the most severe challenges to the use of martensitic steels and vanadium alloys in fusion structures. Therefore, reliable methods must be developed to predict toughness as a function of temperature (T) throughout service. Methods of measuring $K_e(T)$ must also be closely coupled to the analytical procedures used to specify safe operating limits. Developing a $K_e(T)$ data base will, in large part, rely on small specimen testing.

A particular, albeit not unique, challenge of using body centered cubic (bcc), tempered martensitic steels and vanadium alloys is related to the fact that their $K_e(T)$ increases from a lower shelf to a (quasi-) upper shelf over a temperature range defining a brittle-to-ductile transition. Except in very restricted cases, $K_e(T)$ is not a fundamental, unique material property. In particular, $K_e(T)$ depends on size scales, geometry and loading rates, as well as the alloy microstructure, which is modified by irradiation and other characteristics of the service environment.

Figure 1 illustrates the general features of a prototypical $K_e(T)$ curve and the associated stress (σ) displacement (Δ) curve. In the lower shelf and knee region, fracture occurs by a brittle cleavage (or intergranular) mechanism. Up to toughness levels of about $60 \text{ MPa}\sqrt{\text{m}}$ the macroscopic fracture is linear elastic; that is, the fracture stress (σ_f) is less than or close to the general yield stress of the specimen or structure (σ_{gy}), which is geometrically related to the uniaxial yield stress (σ_y) of the alloy. In restricted cases, $K_e(T)$ can be specified as a material property; namely, the linear elastic fracture toughness (K_{Ic}). However, operating safety-sensitive components in a brittle regime is sometimes not acceptable. Fracture also occurs by cleavage initiation in the transition region between about 60 and $175 \text{ MPa}\sqrt{\text{m}}$. However, macroscopically this takes place after general yielding at a finite plastic displacement (Δ_f). Again in restricted cases, $K_e(T)$ can be specified in terms of an elastic-plastic material property, $K_{Jc} = \sqrt{E'J_{Ic}}$, where E' is the plane strain elastic modulus and J_{Ic} is the critical crack tip energy release rate. For cleavage

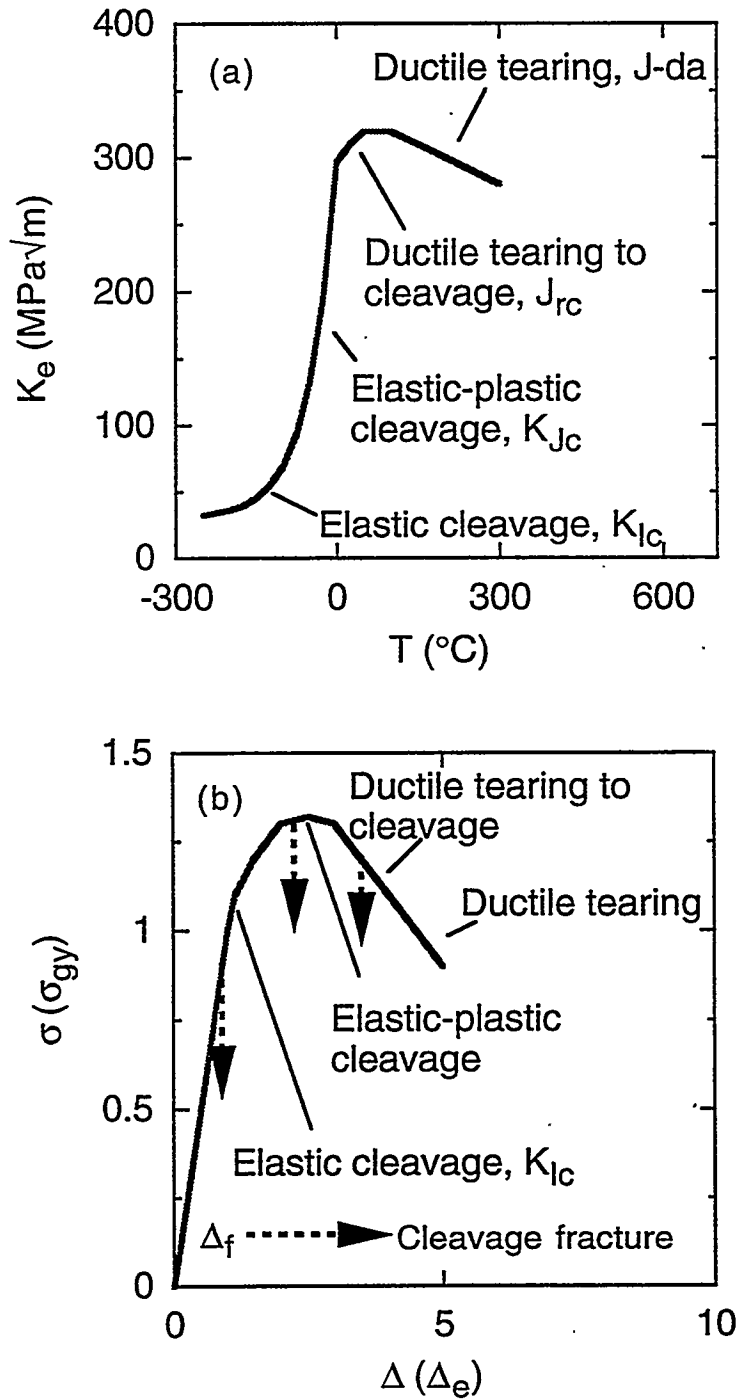


Figure 1 Schematic illustration of a) a $K_e(T)$ curve showing various fracture regimes; and b) the corresponding macroscopic applied stress-deflection (or strain) curve for a test specimen or structure.

initiation, J_{IC} is the area under the stress-displacement curve. It is notable that in this regime, while the microscopic fracture mechanism is by propagation of brittle cleavage cracks, the structure possesses the key engineering property of ductility; and that the major benefit of plastic fracture is the capacity to "bend-before-breaking" rather than a significantly increased load bearing capacity. At still higher temperatures in the transition regime, fracture may occur by ductile tearing preceding a transition to cleavage; and in the quasi-upper shelf regime, fracture occurs by instability of ductile tearing cracks. In this work the focus will be on cleavage initiation, since for most fusion applications ductile tearing can be considered a safe, high ductility regime.

Thus the key question is how to obtain appropriate measures of $K_e(T)$ for cleavage initiation that can be applied to predict σ_f and Δ_f in actual structures. Since irradiation has profound and complex effect on $K_e(T)$, such measurements will inevitably require the use of small specimens. Further, most fusion structures themselves will not have typical heavy section (pressure vessel) configurations, with potentially deep cracks that can make direct use of traditional measures of toughness (i.e., K_{IC} , K_{Jc}). In the past, advanced methods have been proposed based on the concept of local fracture mechanics, which will be described briefly below¹⁻⁸.

However, a much simpler master curve (MC)-temperature shift (ΔT) method is developed here that not only directly links to specifying engineering design and operation limits, but also is compatible with a more fundamental mechanism-based approach. Note, the MC- ΔT method is conceptually similar to the K_{IR} reference curve indexed by Charpy/drop weight nil-ductility transition temperature currently used to regulate nuclear reactor pressure vessels (RPV)⁹. However, the MC- ΔT procedure proposed here is much more physically meaningful, and is specifically pertinent to fusion applications. A variety of F82H data are used to test the feasibility of the method. Note, corollary approaches are under development for RPV applications^{10,11}.

The specific objectives are to:

- 1) Evaluate the effect of specimen width (W), crack length (a) to W ratio (a/W) and loading rate on $K_e(T)$ in unirradiated F82H to assess the possibility of establishing a MC characterized by a specified reference shape that is positioned (indexed) on an absolute temperature scale by a reference temperature (T_0) plus temperature shifts (ΔT) to account for the variables noted above.
- 2) Interpret the fundamental basis for the observed behavior using physically-based micromechanical models and concepts.
- 3) Extend the results to the effects of irradiation induced shifts in miniaturized Charpy V-notch energy (E)-temperature (T) curves for F82H and similar 8 Cr martensitic alloys.
- 4) Illustrate how the method can be applied.
- 5) Identify unresolved issues.

$K_e(T)$ CURVES FOR F82H

A significant body of data on low alloy RPV steels suggest that their $K_{Jc}/J_{IC}(T)$ curve has a relatively constant shape^{10,11}. Thus unirradiated alloys can be placed on an absolute scale by measuring the temperature (T_0) at a reference mean toughness level. For RPV steels, the reference K_{Jc} is typically 100 MPa \sqrt{m} . Further, it has been argued that the effects of irradiation can also be treated as temperature shifts (ΔT_i) measured at the reference toughness level. This so-called master curve (MC) approach also accounts for the inherent large scatter in the transition region using Weibull statistics to set lower bound confidence

limits. This statistical interpretation also leads to size corrections, where K_{Jc} varies with the length of the crack front (B) as $B^{-1/4}$.

Figure 2 plots absolute $K_e(T)$ for F82H which has been presented previously^{4,5}. Two limiting cases are shown: a) a dynamically loaded, deeply pre-cracked ($a/W = 0.5$) Charpy specimen (DPCC); and b) a statically loaded shallow pre-cracked ($a/W = 0.2$) minicharpy (1/3 sized) specimen (SPCMC). The SPCMC is shifted significantly downward in temperature relative to the DPCC data. However, an "eyeball" examination suggests that the two data sets can be superimposed in the lower shelf and transition regions by a ΔT of about 140°C, suggesting the possibility of a MC for F82H.

To further test this hypothesis, Figure 3 plots K_e on an adjusted temperature scale (T') for a variety of specimen configurations and dynamic versus static loading rates. The $T' = T - \Delta T$ is adjusted by the shifts (ΔT) estimated at a reference K_e of 60 $\text{MPa}\sqrt{\text{m}}$ relative to the curve for deeply pre-cracked Charpy (PCC) test with $T_0 = -115^\circ\text{C}$. A value 60 $\text{MPa}\sqrt{\text{m}}$ was chosen for referencing, since it is close to the maximum temperature of elastic fracture in PCC and deeply pre-cracked minicharpy (PCMC) tests; hence, the data are believed to be approximately "valid" even for the small "atypical" specimens used in this study. The ΔT are given in Table 1.

Table 1 -- Values of ΔT at 60 $\text{MPa}\sqrt{\text{m}}$ for Tests on F82H With Various Specimen Configurations and Loading Rates

Specimen/loading rate		$\Delta T(^{\circ}\text{C})$
Shallow pre-cracked minicharpy	(SPCMC)	-60
Shallow pre-cracked Charpy	(SPCC)	-55
Deeply pre-cracked minicharpy	(PCMC)	-20
Deeply pre-cracked Charpy	(PCC)	0 (reference)
0.6T bend bar (about 3x Charpy size)	(0.6TBB)	+10
Dynamic deeply pre-cracked minicharpy	(DPCMC)	+50
Dynamic deeply pre-cracked Charpy	(DPCC)	+80

Figure 3 also shows the recommended MC for RPV steels with a 60 $\text{MPa}\sqrt{\text{m}}$ reference T_0 of -115°C . The RPV MC is given by

$$K_e(T') = 30 + 30\exp[A(T'-T_0)] \quad (\text{MPa}\sqrt{\text{m}}) \quad (1)$$

where $A = 0.019$. Note, the data for the all the PCMC specimens and the SPCC are grossly invalid (K_e is not a material property like K_{Ic} or K_{Jc}) from a standard fracture mechanics perspective at levels above about 100 $\text{MPa}\sqrt{\text{m}}$. The data for PCC are reasonably valid up to about 175 $\text{MPa}\sqrt{\text{m}}$. In spite of these specimen limitations and differences in the steels, however, the RPV MC reasonably represents the F82H $K_e(T)$ trends. Adding a $+30^\circ\text{C}$ margin, shown as the dashed line, approximately bounds the entire data set.

However, closer examination of the data shows that the transition is somewhat steeper for F82H than predicted by the RPV MC, particularly for the specimens that are: very small; and/or have shallow cracks; and/or are dynamically loaded. This is illustrated in Figure 4 where data for these 'atypical' specimens/ tests are shown as circles, while the squares represent more "standard" PCC and 0.6TBB tests. The latter

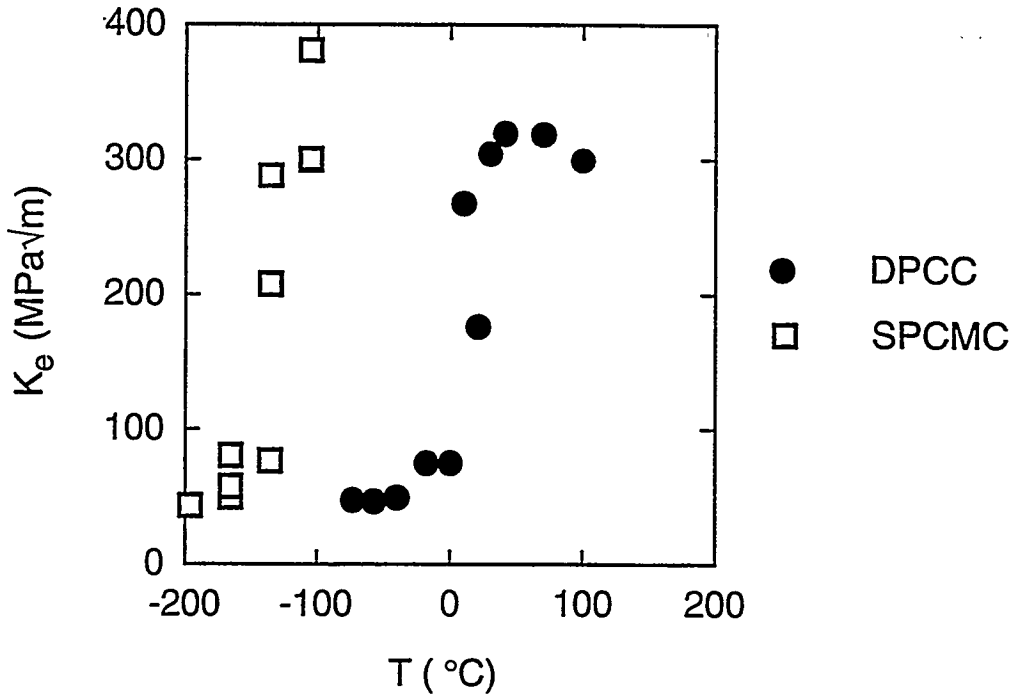


Figure 2 Comparison of the $K_e(T)$ curves for the SPCMC (squares) and DPCC (circles) tests.

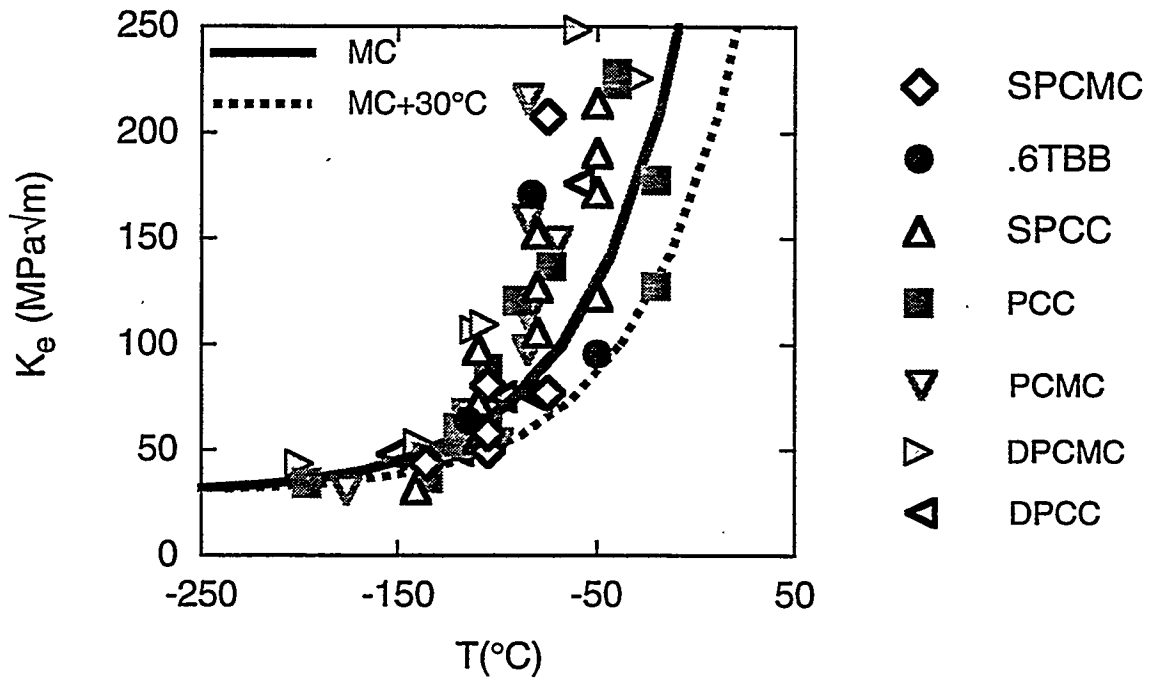


Figure 3 The adjusted $K_e(T)$ curves compared to the RPV MC and MC + 30°C bound.

data tend to follow the RPV MC, although the transition may be a little steeper even in this case. The dashed curve shows a crude fit to the data for the atypical specimens/tests, where the exponential coefficient in Equation 1 has been increased to $A = 0.038$.

Both the shape differences and the shifts shown in Table 1 can be qualitatively understood in terms of the underlying micromechanics of cleavage and the brittle-to-ductile transition. Further, these concepts can be used to model the effects of irradiation and other in-service degradation processes.

LOCAL FRACTURE MECHANICS, CRACK BLUNTING AND MICROMECHANICS MADE SIMPLE

The underlying assumption of traditional fracture mechanics is that the crack tip fields that cause fracture are the same in a specimen as a structure, and can be fully characterized by a single macroscopic loading parameter (K or J)¹². Further, cleavage fracture and the brittle-to-ductile transition in body centered cubic alloys can be explained as follows: a) fracture is caused by the concentrated stress and/or strain fields that develop in the vicinity of an initially sharp fatigue crack as it blunts to a tip opening (δ) in response to externally applied loads; b) fracture occurs at a critical opening (δ_{IC}); c) δ can be related to the external loading conditions, hence, the applied J or K (and δ_{IC} to K_{IC} or J_{IC}); d) the relationship between K , J and δ depends on the alloy stress-strain or constitutive properties (e.g., $\delta/J = 0.5\sigma_y$) and the specimen/structure-crack geometry; e) in limited cases for deep-through (versus surface) cracks in sufficiently large specimens (all dimensions more than about $100\delta_{IC}$), local tip small scale yielding (SSY) stress and strain fields are totally dominated by the nearby crack and are self-similar (e.g., the amplitudes of the stress and strain distributions do not change with δ and the spatial extent of these fields is normalized by δ); f) cleavage requires very high local stresses normal to the fracture plane (σ_n) operating over a microstructurally relevant region ahead of the crack tip (note, it is this stressed area/volume requirement that establishes the physical size scaling in cleavage fracture processes); g) high σ_n requires a combination of a large tensile flow stress which is further elevated by the multiaxial constraint near the crack tip ($\sigma_{nmax} \geq M\sigma_y$, where σ_y is the yield stress and M is a strain hardened constraint factor ≥ 3); h) in bcc alloys large σ_y (used here as a surrogate for flow stress) increases with decreasing T and increasing strain rate ($\dot{\epsilon}$); i) hence, cleavage is promoted by low T and high $\dot{\epsilon}$; j) if the required σ_n -stressed regions condition is not achieved, ductile fracture occurs by strain-controlled, stress-mediated nucleation, growth and coalescence of microvoids that form on hard particles.

While more complex descriptions have been proposed, these ideas can be further quantified by a simple model which postulates that cleavage occurs when the σ_n exceeds a critical local stress (σ^*) over a critical area (A^*) in front of the crack tip, where the σ^*/A^* properties are approximately independent of temperature, strain rate and irradiation. The stressed area (A) can most simply be defined by the isostress contour of σ_n . Under SSY conditions A is proportional to the square of the applied J or δ . The σ^*/A^* condition occurs when the $J/K/\delta$ reach critical values $J_{IC}/K_{IC}/\delta_{IC}$.

These ideas directly explain the ductile-to-brittle transition. At very low temperatures σ_y is high and A^*/σ^* is achieved at a small δ_{IC} . On the lower shelf $K(T)$ is roughly constant due to the fact that there is an approximately equal trade-off between the increased magnitude of σ_n and a decreased size of the stress field with higher σ_y (lower T). However, as σ_y continues to decrease with increasing T , the δ_{IC} required to produce σ^*/A^* begins to increase rapidly. At even higher T , σ_{nmax} is less than σ^* , thus cleavage fracture cannot occur. The effects of loading rate on the position the $K_e(T)$ curve can be simply understood based on the increase of σ_y with $\dot{\epsilon}$. The sharper transition in the dynamic loading tests can also be partly explained on the basis of adiabatic heating in the plastic zone which locally decreases σ_y .

Unique, self-similar relations between σ^*/A^* and δ_{IC} occur only for SSY conditions, which are not maintained in small or shallow cracked specimens. In small specimens σ_n decreases due to a loss of

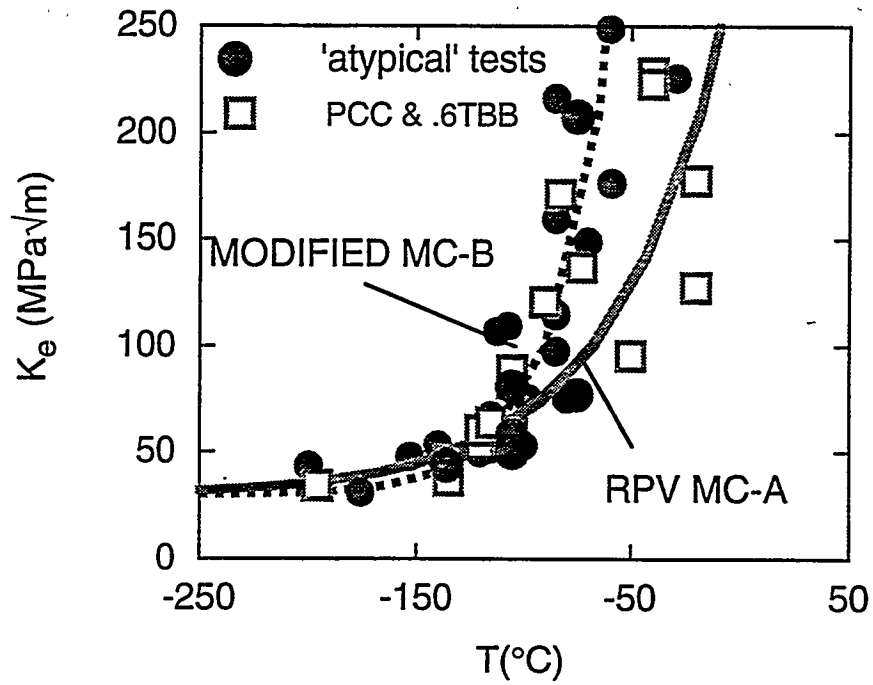


Figure 4 The $K_e(T)$ data for atypical tests (circles) versus PCC and 0.6TBB data (squares) along with the RPV MC (A) and modified MC (B).

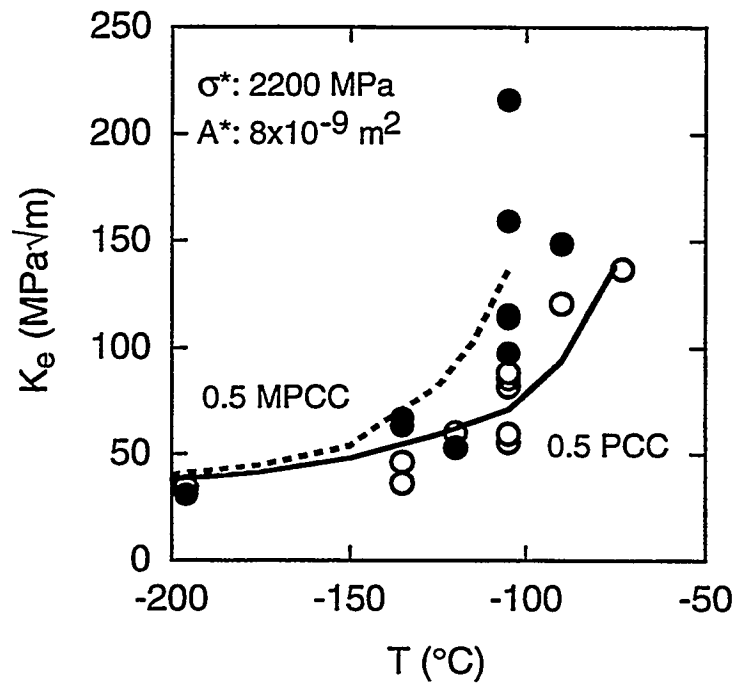


Figure 5 $K_e(T)$ curves predicted by the σ^*/A^* model compared to data for PCMC and PCC specimens.

constraint (lower M) when plastic deformation reaches free surfaces. Likewise for shallow cracks, σ_n decreases due to a constraint reduction caused by secondary non-singular compressive stress fields (so-called T-stresses) in the direction of the specimen width. In both cases, a larger δ_{IC} is needed to achieve the A^*/σ^* cleavage condition. Thus for small and/or shallow cracked specimens the $K_e(T)$ curves are shifted to lower temperature, where the higher σ_y offsets the effects of lower constraint. The somewhat steeper transition in these cases can be explained by a combination of three effects: a) $d\sigma_y/dT$ is higher at lower temperature; b) $\delta(A^*/\sigma^*)$ increases with δ , viz., an initial loss of constraint leads to even more loss of constraint before fracture; and c) loss of lateral plane strain conditions at larger deformation.

Constraint loss retards microvoid nucleation and growth, hence, also increases the ductile fracture toughness. Ultimately small specimens lose the capacity to fracture at all and simply respond to applied loads by massive deformation and crack blunting. Thus great caution must be used in interpreting small specimen data. Small specimens can not only lack the ability to provide "valid" intrinsic properties, but may also fail to detect real physical phenomena such as cleavage or even any type of fracture.

MODELS OF TEMPERATURE SHIFTS DUE TO SIZE, GEOMETRY, LOADING RATE AND IRRADIATION

It has been previously shown that the qualitative concepts described in the previous section can be used to qualitatively model the effects of size, geometry, loading rate and irradiation on both $K_e(T)$ data (only up to a point) as well as Charpy V-notch (CVN) energy-temperature (E-T) curves for both RPV steels and a 12 Cr martensitic stainless steel (HT9)¹⁻⁸.

Application of an A^*/σ^* model to predict size effects in F82H is shown in Figure 5. Here, crack tip stress fields, represented in terms of $A(\sigma_n)$ versus K_I , were computed with the finite element method (FEM) code ABAQUS using an experimentally derived constitutive law. Figure 5 shows the predicted $K_e(T)$ curves for the deeply cracked PCC and PCMC are consistent with the data trends for fixed A^* and σ^* values of $8 \times 10^{-9} \text{ m}^2$ and 2200 MPa, respectively. The predicted ΔT at $60 \text{ MPa}\sqrt{\text{m}}$ of about 25°C is in good agreement with the estimated shift of about 20°C . The same model also correctly predicts that the $K_e(T)$ for specimens with shallow cracks are shifted to lower temperatures, have steeper slopes in the transition region and manifest smaller SPCMC to SPCC shifts than the corresponding curves for the deeply cracked specimens. However, using the same A^*/σ^* of $8 \times 10^{-9} \text{ m}^2/2200 \text{ MPa}$ does not yield good quantitative agreement between the model and the shallow crack $K_e(T)$ data. Thus a simple local fracture toughness model (fixed A^*/σ^*) appears sufficient to treat the gross effect of size, but not crack depth. More detailed micromechanical models are needed to resolve this issue.

The effects of loading (strain) rate ($\dot{\epsilon}$) and radiation hardening ($\Delta\sigma_i$) can be treated even more simply based on the assumption that the maximum temperature of elastic fracture (T_0 at $60 \text{ MPa}\sqrt{\text{m}}$ for static and dynamic toughness) occurs at a specified σ_y . Assumptions of this simple equivalent yield stress (EYSM) model include: a) the overall stress-strain curve is the same at the same σ_y , independent of $\dot{\epsilon}$ and $\Delta\sigma_i$; b) the local fracture conditions (A^*/σ^*) are independent of T , $\dot{\epsilon}$ and irradiation; c) $\Delta\sigma_i$ is independent of T and $\dot{\epsilon}$; and d) T_0 is at about 10J for standard and 0.5J for miniaturized Charpy tests.

First consider shift due between dynamic (d) and static (s) loading rates (ΔT_d). The EYSM states that $\Delta T_d = T_d - T_s$ where $\sigma_{yd}(T_d) = \sigma_{ys}(T_s)$. The effect of $\dot{\epsilon}$ on σ_y can be treated in terms of a strain rate compensated temperature ($T_{s/d}$) as

$$\sigma_y(T_{s/d}, \dot{\epsilon}_{s/d}) = \sigma_y(T_r, \dot{\epsilon}_r) \quad (2a)$$

where,

$$T_r = T_{s/d} [1 + C \ln(\dot{\epsilon}_r/\dot{\epsilon})] \quad (2b)$$

Here T_r and $\dot{\epsilon}_r$ are the reference temperature ($^{\circ}\text{K}$) and strain rate; for F82H, $\dot{\epsilon}_r$ was taken as $3.33 \times 10^{-3}/\text{s}$ and $C \approx 0.028^8$. Thus ΔT_d is simply given by

$$\Delta T_d = T_{os} \{ [1 + 0.028 \ln(\dot{\epsilon}_r/\dot{\epsilon}_s)] / [1 + 0.028 \ln(\dot{\epsilon}_r/\dot{\epsilon}_d)] - 1 \} \quad (3)$$

where T_{os} is the 60 MPa $\sqrt{\text{m}}$ reference temperature for the static tests. The estimated static strain rates for PCC and PCMC are about 7.7 and $23.1 \times 10^{-3}/\text{s}$, respectively. The ratio of the dynamic to static time to fracture is typically about 1.67×10^{-4} . The predicted (ΔT_{dp}) versus measured (ΔT_{dm}) shifts for the PCC and PCMC specimens are shown in Table 2.

Table 2 - Predicted vs. Measured Static to Dynamic ΔT_d

Specimen	T_{os} ($^{\circ}\text{C}$)	ΔT_{dp} ($^{\circ}\text{C}$)	ΔT_{dm} ($^{\circ}\text{C}$)
PCC	-115	75	80
PCMC	-135	65	70

The EYSM can also be applied to the shifts (ΔT_i) due to irradiation hardening ($\Delta \sigma_i$). In this case the shift ΔT_i in the irradiated (T_{oi}) versus unirradiated (T_{ou}) reference temperature is simply given by the condition that $\sigma_y(T_{oi}) = \sigma_y(T_{ou}) + \Delta \sigma_i$. Unfortunately, there is no irradiated $K_e(T)$ data available for F82H. However, the model can be applied to RPV steels as illustrated in Figure 6. Here tests were on PCMC specimens of a A533B reference steel plate (HSST-02) irradiated at 288°C to about 0.04 displacements-per-atom (dpa), producing a $\Delta \sigma_i \approx 155$ MPa. The model predicts a reasonable ΔT_i of about 90°C . However, the predicted decrease in the $K_e(T)$ slope in the transition region is not observed. Further, the EYSM predicts that the $\Delta T_i/\Delta \sigma_i$ ratio (S) increases with increasing $\Delta \sigma_i$ and T_{ou} . Indeed, at very high $\Delta \sigma_i/T_{ou}$ combinations, the model suggests that S increases rapidly above "normal" values in the range of $0.7 \pm 0.4^{\circ}\text{C}/\text{MPa}$. However, large reductions in slope and S values much greater than 1 have not been observed in RPV steels. Hence, as in the case of shallow cracks, more detailed micromechanical models are needed to resolve this apparent limitation of the EYSM.

The EYSM has been successful in using $\Delta \sigma_i$ to predict ΔT_i measured in standard Charpy V-notch tests¹. Application to data reported by Klueh on miniature Charpy V-notch (MCVN) tests on two 9Cr based alloys, similar to F82H, irradiated at 375°C to 7 dpa¹³ is shown in Table 3. The static $\sigma_y(T)$ data is represented by a polynomial given elsewhere⁸. The $\dot{\epsilon}$ for the MCVN tests is taken at 275/s. While the predictions of ΔT_i for the 9Cr-2VWtA alloy are somewhat greater than observed values, the results support the very low embrittlement sensitivity of these alloys, and suggest that this is in part due to the very low T_{ou} .

Figure 7 shows the EYSM applied to some recent data for irradiation of F82H MCVN specimens to 0.8 dpa at 250°C reported by Rieth and co-workers¹⁴. The 0.5J reference T_{ou} was estimated as -90°C , based on MCVN data for F82H⁵. The $\Delta \sigma_i$ are values for dynamic yield stress changes at 100°C . The measured ΔT_i were taken at the reported shifts referenced at 50% of the upper shelf energy, rather than at 0.5J. Good agreement between the measured and predicted ΔT_i is observed.

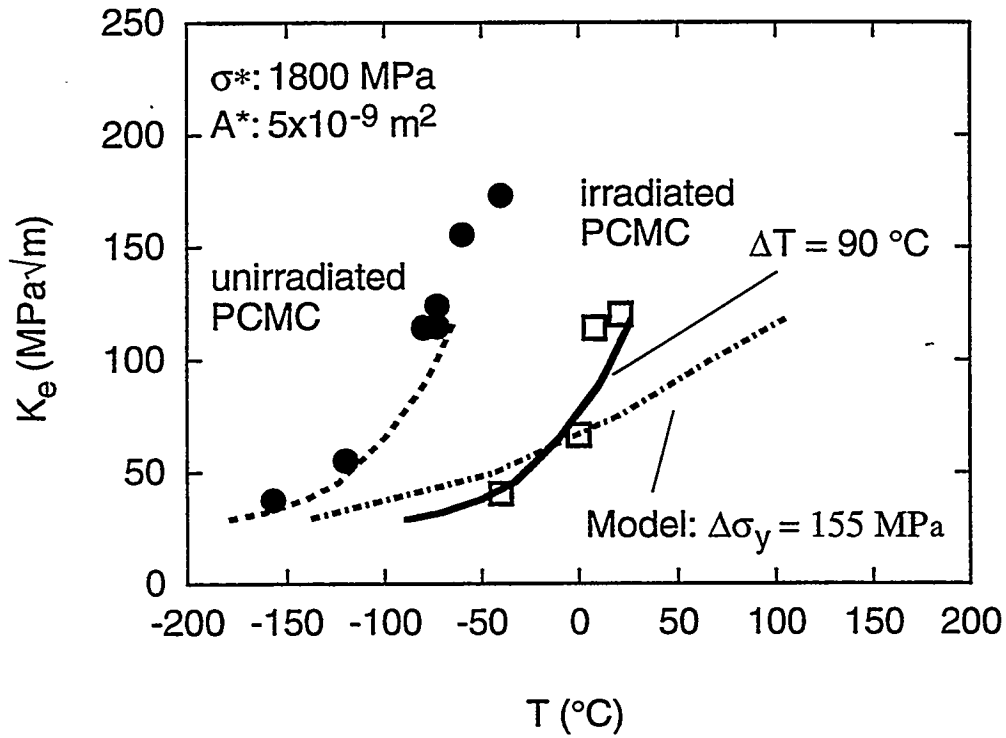


Figure 6 Predicted versus measured shifts in the PCMC $K_e(T)$ curve for an A533B RPV steel due to irradiation resulting in $\Delta\sigma_i$ of 155 MPa.

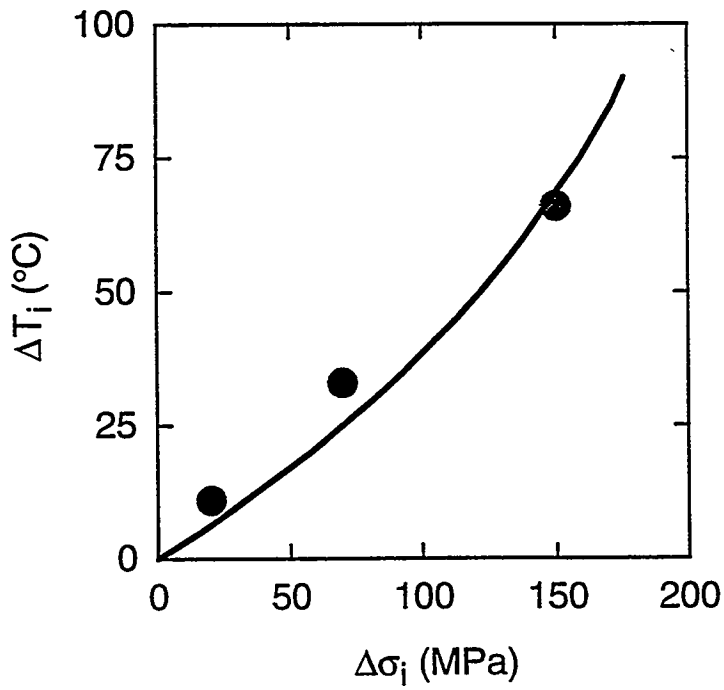


Figure 7 EYSM prediction of ΔT_i as a function of $\Delta\sigma_i$ compared to MCVN data on F82H.

Table 3 - Predicted vs. Measured ΔT_i for MCVN Tests on 9 Cr Steels

Spec./Prop.	T_{ou} (°C)	$\Delta\sigma_i$ (MPa)	ΔT_{ip} (°C)	ΔT_{im} (°C)
9Cr-2VW	-120	161	68	68
9Cr-2VWTa	-150	125	36	11

Overall, the results described in this section demonstrate that application of the simple micromechanical models to F82H qualitatively, and in some cases quantitatively, rationalize the effects of size, geometry and strain rate on $K_e(T)$ curves; and also reasonably predict ΔT_i measured in MCVN tests. In addition, as noted previously, elaboration of the simple models can be used to predict statistical confidence limits and the effects of size scales on the statistics. For example, the slope of 4 assumed (and often observed) in Weibull rank probability versus K log-log plots^{10,11} is consistent with the σ^*/A^* model where the stressed area (A) varies as K^4 under SSY conditions; the scaling of A with K^4 under SSY, also rationalizes the $B^{-1/4}$ dependence on the crack front length, assuming cleavage fracture actually depends on a net stressed volume, rather than area.

The most notable deficiencies in these models are inadequate treatment of shallow versus deep cracks and possible conservative predictions of the effects of irradiation on shifts and shape changes in $K_e(T)$ curves. Predictions of the EYSM are also very sensitive to the value of T_0 which may be difficult to accurately define, particularly for CVN and MCVN tests. However, these limitations can be addressed by additional fundamental research. Finally, it is important to emphasize that rigorous micromechanical models have importance far beyond analyzing and applying fracture data. In particular, such models would be of immense benefit in linking microstructure to mechanical properties and in helping to guide the rational design of higher performance alloys.

ENGINEERING APPLICATION OF THE MC- ΔT METHOD FOR SETTING STRESS, STRAIN AND OPERATING LIMITS ON FUSION STRUCTURES

It is axiomatic that fusion structures will operate under a wide range of conditions of temperature, loading and flaw configurations. Thus design procedures and the supporting data base must be sufficiently general and quantitative to reliably specify safe stress and strain limits for a variety of circumstances, including abnormal events, such as plasma disruptions.

Since fusion reactors will undoubtedly go through many cycles of startups and shutdowns, as well as sustained operation, an analogy to the so called operating-curves for RPVs may be warranted. The RPV operating-curve specifies the combination of pressures (P) and T (P - T) that insure against fracture of the vessel. At low T the allowed P is low since the toughness is low. However, as long as the actual P - T combination is held below the prescribed P - T curve, the vessel is considered safe, even at low K_{Ic} . As the T and K_{Ic}/J_{Ic} increases, the safe operating P also increases. Thus the vessel can be brought from cold-shutdown to hot-operation as long as the primary cooling system can provide enough heat (by pumps in pressurized water reactors) to remain below the P - T curve. However, irradiation-induced shifts in toughness shift the P - T curve up in T , and a very large ΔT may even close the operating window. Other RPV analogies that may be pertinent to fusion structures are treatment of transient events such as pressurized thermal shock.

It is possible to determine the stress-strain limits for fusion structures by appropriate mechanics analysis if the $K_e(T)$ and the basic constitutive properties of a structural alloy are known. In addition to use of

advanced FEM methods, sophisticated non-destructive examination methods will certainly play a key role in assuring the reliability of fusion structures. However, in the following discussion the use of the MC- ΔT method is demonstrated with a very simple example, for purposes of illustration only.

First it is assumed that the two basic shapes shown in Figure 3 can be used as provisional MC [$K_{mc}(T')$] for two classes of application: MC-A for static loads with fracture in or near the SSY regime for sufficiently large dimensions and deep cracks, with $A = 0.019$; and MC-B for high loading rates, shallow cracks and applications involving small dimensions when cleavage fracture occurs well beyond the SSY, with $A = 0.038$.

Figure 8 shows estimates of various stresses for a shallow surface crack ($a/W \approx 0.3$) in a relatively thin ($W = 1.0$ cm) plate with a surface length ($2c$) three times the crack depth ($2c/a = 3$) subject to a rapid disruption stress peaking in about 1 ms (typical of dynamic tests). Hence, MC-B is used in the form

$$K_e(T) = 30 + 30\exp[0.038(T - \Delta T_t - T_0)] \quad (\text{MPa}\sqrt{\text{m}}) \quad (4)$$

where ΔT_t is the total shift accounting for size (ΔT_s), loading rate (ΔT_d), crack depth ($\Delta T_{a/W}$), irradiation (ΔT_i) and a safety margin (ΔT_m). The values used in this example are shown in Table 4.

Table 4 - ΔT Values Used in the MC- ΔT Application Example

Adjustment	Temperature/Shift($^{\circ}\text{C}$)
T_0	-115
ΔT_s	+10
ΔT_d	+80
$\Delta T_{a/W}$	-20
ΔT_i	+100, 200, 300
ΔT_m	+60

The solid curves are the estimates of the stresses at cleavage initiation based on a elastic stress intensity factor and ΔT_i of 100, 200 and 300 $^{\circ}\text{C}$ (indicated respectively by the increasing line thickness). The dashed curves are the unirradiated static and dynamic σ_y (σ_{ysu} , σ_{ydu}) and σ_{ysi} is simply the σ_{ysu} increased by an arbitrary $\Delta\sigma_i = 300$ MPa. The results show that for $\Delta T_i = 300^{\circ}\text{C}$ the structure is brittle at operating temperatures below about 260 $^{\circ}\text{C}$ and must be operated at a value well below σ_{ysu} . At higher operating temperatures, the stress limits may increase slightly above σ_{ysu} (e.g., $\approx 20\%$); however, since the stress capacity of the structure is ultimately limited by deformation controlled collapse (rather than fracture), higher temperatures are significant primarily in increasing the structures ductility. Sufficient ductility is very important since it reduces the effects of secondary (self-relieving) stresses, and also enables the stress reductions provided by typical structural compliance. Of course, what constitutes sufficient ductility depends on the specific design. The minimum temperature of the ductile regime varies directly with ΔT_i .

Figure 8 can also be viewed as an example of an operating curve. Consider the following set of scenarios (again, as examples only). At startup in the brittle regime the primary stresses (σ_p) and thermal (or residual) stresses (σ_{th}) might be limited to

$$\sigma_p + \sigma_{th} < 0.33\sigma_{max} \quad (5a)$$

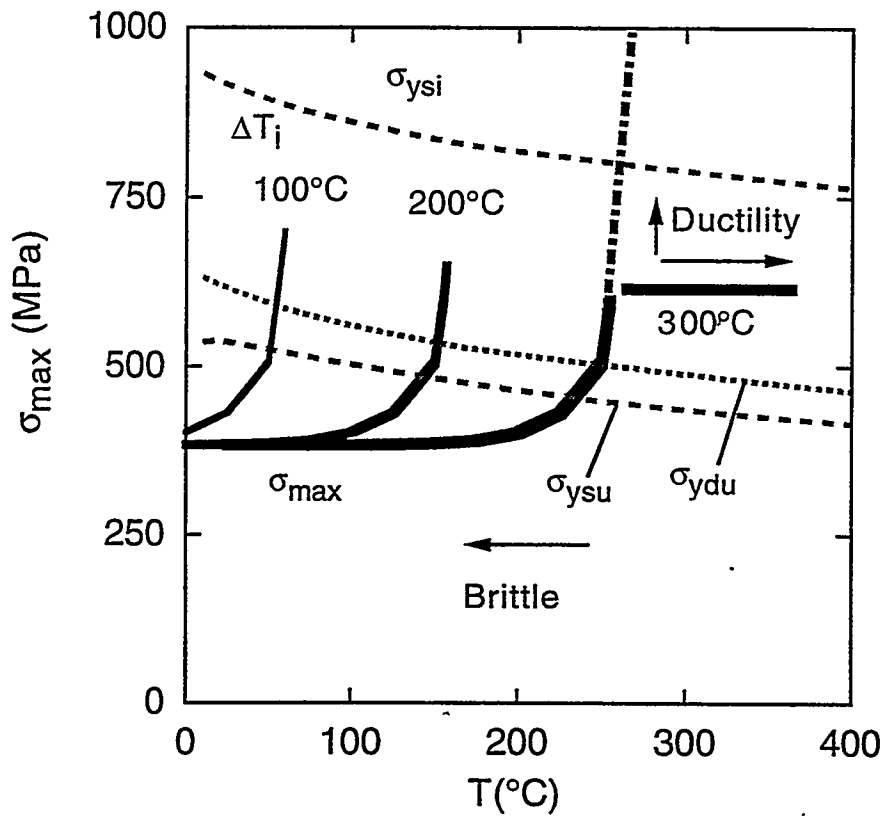


Figure 8 A schematic illustration of how the MC- ΔT method could be used to establish maximum operation stress-temperature limits in a fusion reactor structural component. At low temperatures in the brittle regime the stresses would be limited to a small fraction of the σ_{ysi} . At higher temperatures above the transition, the stress limits could be increased, depending on the structural ductility requirement. In the ductile regime the maximum stresses would be limited to the σ_{ydu} unless credit were taken for the $\Delta\sigma_i$.

giving a safety factor of 3. This might be managed by controlling the heating rate and the coolant pressure. At higher operating temperatures, in the ductile regime, the allowed stress limits might be increased to something like,

$$2\sigma_p + \sigma_{th} < 0.9\sigma_{ysu} \quad (5b)$$

giving a safety factor of 2 for primary stresses and 1 for thermal stresses. Finally, during a rare transient the safety margins might be further relaxed to

$$\sigma_p + \sigma_{th} < 0.9\sigma_{ysu} \quad (5c)$$

While these results are not numerically significant, they illuminate a key point. That is, unless an appropriate data base and closely coupled fracture mechanics method are available, it will not be possible to design a fusion reactor structure that can be licensed and operated in a safe, efficient and reliable manner. Clearly, a key element of this is an appropriate data base on irradiation embrittlement. Hence, it is particularly unfortunate that previous, ongoing and most planned irradiation programs will collectively provide only very limited information necessary to accomplish this objective.

USE AND MISUSE OF SMALL SPECIMEN TESTS

The technical conclusions of this work point to the need for a significant modification of current approaches to irradiation experiments in particular, and methods of dealing with embrittlement in general. Hence, while the author does not intend that the following statements be viewed as being too harsh or overly critical, given the costs, time and often one-of-a-kind nature of irradiation experiments, a wake up call is clearly needed. First, small specimen test methods can and will play a critical role in developing an appropriate embrittlement data base. However, this will be effective if, and only if:

- the small specimen tests are specifically designed to provide a comprehensive range of data including information on size, geometry, loading rate (as well as irradiation effects) on $K_e(T)$ and the basic alloy constitutive properties;
- the small specimen test data are analyzed, interpreted and applied with a sufficient level of understanding of the fundamental micro- and macro-mechanics of fracture;
- the data base is closely coupled to an analytical method to determine the safe stress and displacement (or strain) limits of actual fusion structures.

While these points seem obvious, they have not been generally reflected in the past, current and most planned irradiation experiments. For example, MCVN tests are typically used as the main measure of embrittlement. However, no method has been presented, or proposed, as to how to use this data base to predict the performance of fusion structures. Indeed, it has been argued that the MCVN tests are good "screening tools" that can rank the relative performance of different alloys; however, even this assumption has been shown to be incorrect⁵ (as well as being a limited and dated objective). It is further noted that efforts to relate MCVN to full sized Charpy test results are not useful in this regard. Perhaps an even more egregious shortcoming of these simple-minded approaches is the persistent failure to include sufficient numbers of tensile specimens in key irradiation experiments.

CONCLUSIONS

A practical engineering method for managing the problem of irradiation embrittlement fusion reactor structures based on a master curve-reference temperature shift (MC- ΔT) method has been proposed. A preliminary evaluation of existing data shows the approach to be very promising. In particular, the MC- ΔT method is, on one hand, compatible with quantitative evaluation of stress and strain limits in actual structures while also capable of being interpreted and supplemented by a fundamental understanding of the micromechanics of fracture and embrittlement. The latter is absolutely necessary if small specimen test methods are to be used to develop the necessary embrittlement data base. However, significant research is needed to implement the MC- ΔT method or any other viable alternative. For example, the understanding of fracture due to shallow cracks and the effect of irradiation on the shape of the toughness-temperature curve are currently inadequate. However, the most critical need is to carry out irradiation experiments that will actually be useful in developing a data base for an integrated method of assessing the fracture safe margins of fusion structures.

ACKNOWLEDGMENTS

The contributions of G. Lucas, K. Edsinger, W. Sheckherd and B. Wirth to the research supporting the approach developed in this work are greatly appreciated. The research was supported by the US Department of Energy, Office of Fusion Energy Grant # DE-FG03-87ER-52143.

REFERENCES

1. G. R. Odette, P.M. Lombrozo, P.M., R. A. Wullaert, "The Relationship Between Irradiation Hardening and Embrittlement of Pressure Vessel Steels", *Effects of Irradiation on Materials*, 13, ASTM-STP-870, ASTM (1985) 841.
2. G. R. Odette, "On the Ductile to Brittle Transition in Martensitic Stainless Steels", *J. Nucl. Mater.*, 212-215 (1994) 45.
3. G. R. Odette, B. L. Chao, G. E. Lucas, "On Size and Geometry Effects on the Brittle Fracture of Ferritic and Tempered Martensitic Steels", *J. Nucl. Mater.*, 191-194 (1992) 827.
4. K. Edsinger, G. R. Odette, G. E. Lucas, J. W. Sheckherd, "The Effect of Size, Crack Depth and Strain Rate on the Fracture Toughness-Temperature Curves of a Low Activation Martensitic Stainless Steel", *J. Nucl. Mater.* (in press).
5. G. E. Lucas, G. R. Odette, J. W. Sheckherd, K., Edsinger and B. Wirth, B., "On the Role of Strain Rate, Size and Notch Acuity on Toughness: A Comparison of Two Martensitic Stainless Steels", *Effects of Radiation on Materials*, 17, ASTM STP 1270, ASTM (in press).
6. K. Edsinger, G. R. Odette, G. E. Lucas, B. Wirth, "The Effect of Constraint on Toughness of a Pressure Vessel Steel", *ibid* 5.
7. B. Wirth, K. Edsinger, G. R. Odette and G. E. Lucas, "Evaluation of Embrittlement in a Pressure Vessel Steel by Fracture Reconstruction", *ibid* 5.
8. K. Edsinger, "Fracture Reconstruction and Advanced Micromechanical Modeling of Structural Steels", PhD Thesis - Department of Chemical and Nuclear Engineering, University of California, Santa Barbara (1995)

9. United States Nuclear Regulatory Commission, Regulatory Guide 1.99: Radiation Embrittlement to Reactor Vessel Materials, U.S. Government Printing Office, Washington, D.C. (1988).
10. K. Wallin, "The Scatter in K_{Ic} Results", Engineering Fracture Mechanics, 19-6 (1984) 1085
11. D. McCabe, J. G. Merkle and R. Nanstad, "A Perspective on Transition Temperature and K_{Ic} Data Characterization", Fracture Mechanics, 24, ASTM STP 1207, ASTM (1994) 215
12. D. Broek, Elementary Engineering Fracture Mechanics, Kluwer Academic Publishers (1991)
13. R. Klueh and D. Alexander, "Impact Toughness of Irradiated Reduced Activation Ferritic Steels", Fusion Reactor Materials Semiannual Progress Report 9/30/93 DOE/ER-0313/15 (1994) 148
14. M. Reith, B. Dafferner, H.D. Rohrig, "Charpy Impact Properties of Low Activation Alloys for Fusion Applications After Neutron Irradiation", J. Nucl. Mat. (in press)